

Reports

The Detection of Eclipses in the Pluto-Charon System

Abstract. *The first eclipses between Pluto and its satellite ("Charon") were detected in January and February 1985, confirming the satellite's existence. Eclipses lasting a few hours will now occur at 3.2-day intervals for the next 5 to 6 years and then will cease for about 120 years. Careful observations of these eclipses will allow greatly improved determinations to be made of several physical parameters for the Pluto-Charon system: the diameters of the planet and satellite, the surface albedo distribution on one hemisphere of the planet, the orbit of the satellite, and the mass of the planet and hence its density. Knowledge of the density will provide a constraint on models of Pluto's bulk composition.*

Shortly after the discovery of a satellite of Pluto in 1978 (1), it was noted that a series of mutual eclipses might be observable beginning in 1979 (2). An improved orbit determination revised this estimate to the early 1980's (3). Because these eclipse events are observable for only a short period every 124 years, when Pluto's heliocentric motion causes the plane of the satellite's orbit to sweep across Earth's orbit, their observation offers a rare and unique means to improve our knowledge of this distant planet-satellite system.

We now report the beginning of this long-awaited eclipse series between Pluto and its satellite, officially known as "1978 P1" and unofficially as "Charon" (4). Here we use the word "eclipse" as a general term to refer to both occultations (satellite passing behind the planet) and transits (satellite passing in front of the planet).

Direct detection of Charon from ground-based telescopes is difficult because its maximum apparent separation from Pluto is only about 0.9 arc second. This value is near the limiting angular resolution afforded by Earth's atmosphere at optical wavelengths. Although speckle interferometric techniques have been used to resolve the planet and satellite (5-7), the small apparent sizes of these bodies makes an accurate determination of their physical parameters problematical.

Most of our knowledge of Pluto itself comes from telescopic measurements made with photoelectric detectors. A periodic variation in Pluto's brightness was first noted in the 1950's (8). Measurements and plots of brightness over time (called "lightcurves") have shown that this variation, presently amounting to 30 percent, is periodic over an interval of about 6.4 days due to the planet's

rotation and a nonuniform surface albedo distribution. Eclipse events will be superimposed on this rotational variation. Because the shape and amplitude of Pluto's rotational lightcurve have been slowly changing with time, due to a geometric effect, careful measurements of the rotational lightcurve at the current epoch were needed so that eclipse events could be deconvolved from the intrinsic rotational variations. In anticipation of the onset of eclipses, we have been conducting such studies for several years (9-12).

Our baseline observations of the uneclipsed lightcurve allowed us to make the first positive detections of the predicted eclipses between Pluto and Charon in January and February of 1985 (Table 1 and Fig. 1), even though these events were shallow. The observations on 16 January were made by E.F.T. and B.J.B. with the 1.5-m reflecting telescope at the Mount Palomar Observatory and a charge-coupled device (CCD) detector (13). Each CCD image contained two comparison stars in addition to Pluto-Charon. The integrated flux of the three objects, corrected for instrumental effects and sky background, were then compared to obtain the variation of their brightness with time. The brightness ratio of the two comparison stars was constant to within 0.007 magnitude over the period of observation, while the brightness ratio of the Pluto system and one of the comparison stars varied as shown in Fig. 1 (top plot). However, because of a possible detector problem (14) and the fact that this event occurred about 3 hours (5 σ) earlier than predicted by a preliminary version of the orbit solution (15), these observations were initially uncertain.

On 17 February an eclipse event was detected clearly by R.P.B. at the McDonald Observatory with a photoelectric photometer (10) attached to a 0.9-m cas-

Table 1. Initial eclipse data.

Date of observation		Earth-Pluto distance (AU)	Eclipse parameters		
UT, 1985	Julian date		Phase	Depth (magnitudes)	Duration (hours)
January 16.467	2,446,081.967	29.91	0.251	0.04 \pm 0.01	>1.0
February 17.385	2,446,113.885	29.38	0.248	0.031 \pm 0.005	\sim 2.0
February 20.585	2,446,117.085	29.34	0.750	0.024 \pm 0.004	\geq 2.0

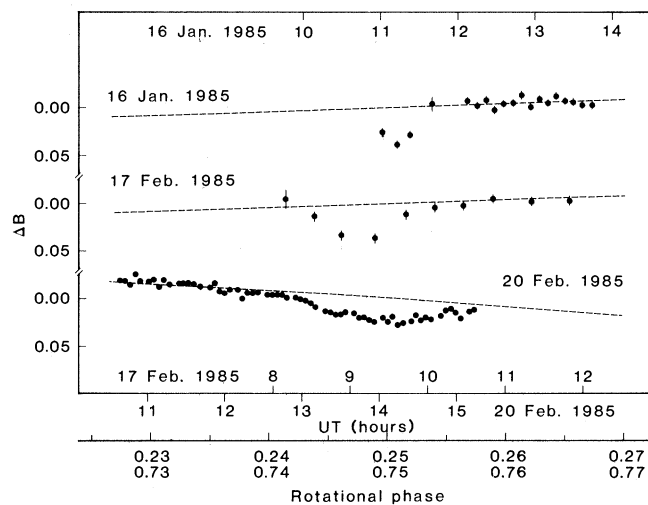


Fig. 1. Lightcurves of the first eclipse events between Pluto and Charon detected in January and February 1985. These lightcurves have been aligned by integer multiples of one-half the satellite's orbital period. All measurements were made in blue light. The mean uneclipsed lightcurve as determined from observations in previous years is indicated by a dashed line. The ordinate (Δm) is in units of magnitudes normalized to the mean uneclipsed light

level at phases 0.25 and 0.75, respectively. The upper two lightcurves correspond to rotational phases near 0.25, and the lower lightcurve corresponds to a phase near 0.75.

segrain telescope. From this detection, it was determined that the 16 January observations showed an excellent correlation with those of 17 February. Thus the January observations represented the first detection of eclipses between Pluto and Charon.

Confirming observations were made on 20 February by D.J.T. at the Mauna Kea Observatory with the University of Hawaii's 2.24-m telescope and a photometer equipped with an RCA C31034A photomultiplier and pulse-counting electronics. The measurements of Pluto-Charon on 17 and 20 February were made differentially with respect to a nearby comparison star (~10 arc minutes away) located at $14^{\text{h}} 29^{\text{m}} 44.6^{\text{s}} +03^{\circ} 04' 03''$ (1950 coordinates) to account accurately for atmospheric extinction. This star was selected in 1984 because of its close color match to Pluto.

The phases for the eclipse events (Table 1) indicate the fractional part of the satellite's 6.38726-day synodic period that has elapsed since a chosen epoch: Julian date 2444240.661 (Plutocentric), a time corresponding to a minimum brightness of Pluto's rotational variation, corrected for the light travel time between Pluto and Earth. At this epoch the satellite was near its greatest northern elongation. (The satellite's orbital period and the planet's rotational period are identical to within the current observational uncertainties, implying that the satellite is in a synchronous orbit.) The phase for any time of observation is indicated by the fractional portion of the number E , computed from Eq. 1.

$$E = \frac{\text{JD} - 0.0058\Delta - 2444240.661}{6.38726} \quad (1)$$

where JD is the Julian date of observation and Δ is the distance between Earth and Pluto in astronomical units (AU).

The two events observed near phase 0.25 are due to partial transits of the satellite across Pluto, and the event near 0.75 is due to a partial occultation of the satellite by Pluto (Fig. 1 and Table 1). Although it would be premature to use these initial observations to refine our estimates of parameters in the Pluto-Charon system, three specific items are worthy of note. The first is the difference in the depths between the 0.25 and 0.75 events. This can be explained most simply by requiring that the portion of Pluto's surface occulted by Charon have a higher albedo than the portion of Charon's surface occulted by Pluto. In this case, although the areas involved are very nearly equal because of the slowly changing geometry, the former event results in a greater diminution in light

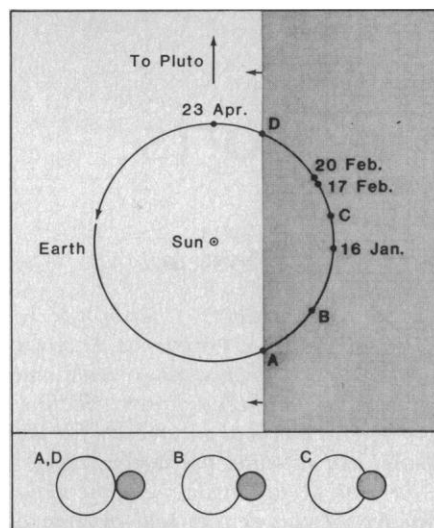


Fig. 2. (Upper panel) The present geometry of the intersection between the ecliptic plane and the penumbral shadow cone (shaded region), showing the locations of Earth on nights when eclipse events were observed as well as Pluto's 1985 opposition date. The diagram illustrates why events are initially seen only near preopposition quadrature. The shadow region is sweeping over Earth's orbit at a rate of about 1.2 AU per year; thus we can expect to observe events well past opposition in 1986. (Lower panel) The configuration for Pluto and Charon as seen at the 0.25 rotational phase for various points (A to D) along Earth's orbit.

because a brighter surface is being obscured. Second, because the events are occurring almost precisely 0.5 phase apart, the orbit of Charon must be very nearly circular, as would be expected from the presumed synchronous orbit. Finally, these eclipse timings and the aforementioned orbital period make possible the accurate prediction of future events.

As indicated above, these initial observations are of partial events between Pluto and Charon. Over the next 5 to 6 years, Charon will appear to pass more centrally in front of and behind Pluto. Thus eclipses will occur twice every orbital period, that is, roughly every 3.2 days. The eclipse lightcurves will continually evolve over this interval as Pluto's heliocentric motion and the annual parallax motion of Earth result in a constantly changing viewing geometry. This implies that frequent observations of the eclipse lightcurves will be necessary to extract all of the information they offer.

The present geometry (Fig. 2) shows the penumbral shadow cone sweeping over Earth's orbit. The exact location of the edge of the shadow is not yet well determined. Also, the diameter of the shadow cone depends on the relative sizes of Pluto and Charon, as well as their separation, and as such is also

poorly determined. The length of the eclipse season is determined by the size of the shadow cone.

Measurements of the true durations and depths of the eclipses as they evolve over the next several years will allow reliable diameters to be determined for both Pluto and Charon. Initial calculations of eclipse lightcurves (which neglect shadowing) (16) assume that Charon is one-half the diameter of Pluto, that the orbital separation is 10 Pluto radii, and that the bodies have equal albedos. This model predicts that a central eclipse will last nearly 5 hours and will reach a depth greater than 0.2 magnitude. Recent calculations by Tedesco that account for shadowing (17) show that this effect will deepen the eclipses to as much as 0.4 magnitude. Eclipse timings will also serve to improve the orbital elements of Charon, which will lead to an accurate determination of the total mass of the system. These diameter and mass determinations will allow a reliable density to be computed for Pluto, from which its composition may be more accurately inferred.

Finally, the eclipse series will provide a rare opportunity to construct an albedo map of one hemisphere of Pluto. This will be possible by making frequent observations of the eclipse lightcurves as Charon transits across slightly different portions of Pluto. Small-scale variations in Pluto's albedo will be detectable as deviations from smooth eclipse lightcurves. The present series of eclipse events will be our only opportunity to measure such markings on the surface of Pluto for many years, since no spacecraft missions to this planet are likely until the next century.

We are coordinating a global campaign to monitor Pluto-Charon eclipses because only about 20 percent of the total number of events will be observable from any single observatory. Observations with 2-m class telescopes at major observatories worldwide are encouraged. By standardizing techniques and reference stars, the scientific return during this once-per-century opportunity can be maximized.

RICHARD P. BINZEL

*Department of Astronomy,
University of Texas, Austin 78712*

DAVID J. THOLEN

*Institute for Astronomy, University
of Hawaii, Honolulu 96822*

EDWARD F. TEDESCO*

BONNIE J. BURATTI*

ROBERT M. NELSON*

*Jet Propulsion Laboratory,
California Institute of Technology,
Pasadena 91109*

References and Notes

1. J. W. Christy and R. S. Harrington, *Astron. J.* **83**, 1005 (1978).
2. L. E. Andersson, *Bull. Am. Astron. Soc.* **10**, 586 (1978).
3. R. S. Harrington and J. W. Christy, *Astron. J.* **86**, 442 (1981).
4. The International Astronomical Union (IAU), as of this writing, has not officially recognized the existence of 1978 P1, although it is expected to do so at the General Assembly meeting in late 1985. Until then, the name "Charon" remains unofficial. In Greek mythology, Charon was the boatman who ferried souls to the realm of Hades across the river Styx; Pluto was, of course, the Roman aspect of the Greek god Hades.
5. E. K. Hege *et al.*, *Icarus* **50**, 72 (1982).
6. G. Baier, N. Hetterich, G. Weigelt, *Messenger* **30**, 23 (1982).
7. D. Bonneau and R. Foy, *Astron. Astrophys.* **92**, L1 (1980).
8. M. F. Walker and R. Hardie, *Pub. Astron. Soc. Pacific* **67**, 224 (1955).
9. E. F. Tedesco and D. J. Tholen, *Bull. Am. Astron. Soc.* **12**, 729 (1980).
10. R. P. Binzel and J. D. Mulholland, *Astron. J.* **88**, 222 (1983).
11. ———, *ibid.* **89**, 1759 (1984).
12. D. J. Tholen and E. F. Tedesco, *Bull. Am. Astron. Soc.* **16**, 923 (1984).
13. T. A. Boroson, I. B. Thompson, S. A. Sheckman, *Astron. J.* **88**, 1707 (1983).
14. At 11:40 UT, it was noted that the dewar was running low on cryogen (liquid nitrogen), at which time it was refilled. The fear that the photometry might have been affected was subsequently established to have been unfounded.
15. A complete description of the orbit solution and its uncertainties may be found in D. J. Tholen, *Astron. J.* (submitted, 1985).
16. J. D. Mulholland and R. P. Binzel, *Astron. J.* **89**, 882 (1984).
17. M. P. Wijesinghe and E. F. Tedesco, *Icarus* **40**, 383 (1979).
18. We thank M. Frueh, K. Amaral, and B. Staples for technical assistance. Supported by NASA grants NGR 44-012-152 (R.P.B.) and NGL 12-001-057 (D.J.T.). A portion of this work was performed at the Jet Propulsion Laboratory, California Institute of Technology, under contract to NASA.

* Guest observer, Palomar Observatory, California Institute of Technology.

10 April 1985; accepted 9 May 1985

Enhanced Immunogenicity of the Pre-S Region of Hepatitis B Surface Antigen

Abstract. *The 55 codons upstream of the gene sequence encoding the hepatitis B surface antigen (HBsAg) are called the pre-S(2) region. It has been proposed that polypeptides of high molecular weight that contain the pre-S(2) region should be included in future hepatitis B virus (HBV) vaccines. The pre-S(2) region and the S gene product [25 kilodalton (kD)] together compose a polypeptide of high molecular weight (33 kD). As an initial attempt to determine the relevance of the 33-kD polypeptide to development of an HBV vaccine, the murine immune response to pre-S(2)-encoded determinants as compared to S-encoded determinants on the same polypeptide was examined. The results indicate (i) the pre-S(2) region is significantly more immunogenic than the S region of HBsAg, (ii) the 26 amino acid residues at the NH₂-terminus of the 33-kD polypeptide represent a dominant antibody binding site on the pre-S(2) region, (iii) the immune response to the pre-S(2) region is regulated by H-2-linked genes distinct from those that regulate the response to the S region, and (iv) immunization of an S region nonresponder strain with HBV envelope particles that contain both the pre-S(2) and S regions can circumvent nonresponsiveness to the S region.*

Immunologic markers of hepatitis B virus (HBV) include the surface antigen (HBsAg), the core antigen (HBcAg), and the core-derived HBeAg. Since HBsAg-specific antibodies are protective against HBV infection, virus-free envelopes present in the plasma of chronic carriers have served as a source of HBV vaccines. The HBsAg is composed of a major polypeptide, p25, and its glycosylated form, gp28 (1). The complete 226 amino acid sequence of the p25 polypeptide of HBsAg has been deduced from partial amino acid sequence data (1) and from the nucleotide sequence of the viral gene (S) that encodes this polypeptide (2-4). Additional polypeptides of higher molecular weight associated with HBsAg have been considered aggregates of p25 and gp28; however, p25 begins at the third possible translational initiation site of a larger open reading frame (ORF) and is preceded in phase by 163 or 174 codons (subtype-dependent) designated

the pre-S region (5). An HBV-associated 33- to 36-kilodalton (kD) glycoprotein (gp33) has been identified (6), and it has been suggested that the sequence of gp33 starts at the second translational initiation signal of the ORF, which is 55 codons upstream from the third signal (7). It has been shown that gp33 consists of the p25 sequence and a sequence of 55 amino acid residues at the NH₂-terminus encoded in this pre-S(2) region (8, 9). In support of this, Neurath and co-workers synthesized a peptide encompassing the 26 amino acid residues at the NH₂-terminus of the pre-S(2) region, and antibodies to this peptide reacted with gp33 (10).

The fact that the pre-S region is conserved in all described HBV DNA sequences and conserved through evolution (11) suggests a functional role for this region. This interpretation is supported by the observation that gp33 appears to be preferentially expressed in viremic carriers as opposed to carriers

with minimal or no infectious virions in the blood (8, 12). This suggests a correlation between viral replication and synthesis of the higher molecular weight polypeptides of HBsAg. Additionally, the receptor for polymerized human albumin, which has been suggested to mediate viral attachment, has been localized on gp33 (13). The implications of these recent findings relative to HBV vaccine development and to mechanisms of immune-mediated viral clearance prompted us to investigate the immune response to the S- and pre-S(2)-encoded gp33 polypeptide of HBsAg.

In previous studies of the murine humoral and cellular immune response to HBsAg, we demonstrated the influence of at least two H-2-linked immune response (Ir) genes and identified HBsAg high-responder (H-2^d and H-2^q), and nonresponder (H-2^f and H-2^s) haplotypes (14-16). The HBsAg used in those studies contained the p25 and gp28 polypeptides but lacked the higher molecular weight polypeptides coded for by the pre-S region, here designated as HBsAg/p25. In the present studies we compared the immune responses to pre-S(2)-encoded determinants and S-encoded determinants of HBsAg in terms of immunogenicity, specificity, H-2-linked regulation, and possible overlapping regulatory mechanisms (that is, whether or not the T-cell helper function generated in response to the pre-S region would influence the anti-S response). For this purpose we used HBsAg particles derived from Chinese hamster ovary (CHO) cells transfected with a plasmid containing the S gene and the pre-S region of HBV (17); these particles are designated HBsAg/p34. The HBsAg/p34 particles are composed of the S-encoded p25/gp28 polypeptides plus the pre-S(2)- and S-encoded gp34 polypeptide. The gp34 polypeptide corresponds to HBV gp33 (17).

Groups of mice from a panel of H-2 congenic strains were immunized intraperitoneally with 1.0 μg of HBsAg/p34 emulsified in complete Freund's adjuvant (CFA). On a weight basis this was equivalent to 0.913 μg of S region protein and 0.087 μg of pre-S(2) region protein per mouse or approximately a tenfold excess of S region protein. Ten days after immunization, all the strains in Fig. 1 contained immunoglobulin G (IgG) specific for the pre-S(2) region polypeptide but none for the S region polypeptide, even though they had received a tenfold greater dose of S region protein than of pre-S(2) region protein. The responses of these strains to a 4-μg dose of HBsAg/p25 are shown with broken lines for comparison (these lines represent re-